

# An Image-encoded Mach-Zehnder Joint Transform Correlator for Polychromatic Pattern Recognition with Multi-level Quantized Reference Functions

Chungcheng Lee, Chulung Chen, Chunmin Wang, and Chiehpo Chang

**Abstract**—The concept of using image-encoded input representation in a Mach-Zehnder joint transform correlator system with multi-level quantized reference functions based on the HSV color space for polychromatic pattern recognition is proposed, in which we present that the large zero order term can be removed in only one step by the Stokes relations. By the image-encoding technique, the size of the liquid crystal spatial light modulators will be less with interlaced rearrangement of hue, saturation and value color components. Simultaneously, multi-level quantized reference functions (MQRFs) which including finite quantization levels are utilized to design the input reference function. Since the reference function is real-valued in the spatial domain, the LCSLM device in the image-encoded Mach-Zehnder joint transform correlator requires only real-valued modulation. Consequently, a reflective LCSLM device (RLCSLMs) also can be utilized to achieve the only real-valued modulation. Computed numerical results are shown to verify the performance of this system.

**Index Terms**—image-encoded Mach-Zehnder joint transform correlator, multi-level quantized reference functions, polychromatic pattern recognition, reflective liquid crystal spatial light modulator.

## I. INTRODUCTION

Increased attention has been focus on liquid crystal spatial light modulators (LCSLMs) in the optical pattern recognition literature in recent years. There are many advantages of using optical techniques with LCSLMs, e.g. capability of high-speed parallel operation, broad-bandwidth, non-crosstalk interconnection, and real-time signal processing. These are useful information for pattern recognition in which a great quantity of data need to be processed. Accordingly, optical correlators have been implemented for pattern recognition. There were two well-known optical correlators for pattern

recognition, which are the VanderLugt (or matched filter based) correlator (VLC) [1] and joint transform correlator (JTC) [2]. Compared with the VLC, because the JTC system does not have the stringent filter-alignment problem, the JTC is more robust in term of environment disturbances and more suitable for real-time processing than VLC. However, the classical JTC has a disadvantage. That is a large zero-order term in the correlation output. The recognition ability of this system will be decreased by the zero-order term. The desired cross-correlation peaks were almost overshadowed and the output detector was often saturated. To remove the zero-order term, many methods have been proposed to accomplish the nonzero order JTC (NOJTC): for instances, phase-shifting technique [3] and joint transform power spectrum (JTSP) subtraction strategy [4]. Nevertheless, the removal of the zero-order term in the NOJTC requires more time-consuming steps. To improve this, Cheng et al. [5] proposed a method that utilized a Mach-Zehnder configuration in the NOJTC (MZJTC), which can remove the zero-order term directly in only one step. Besides, this system does not need to store the Fourier spectra of both the target and reference images in the computer. Accordingly, several research groups have studied to improve the performance of JTC [6]-[8]. For pattern recognition, color is also an importance types in visual information. As a result of the importance of color information, the multi-channel single-output NOJTC [9] system has been proposed by Deutsch et al. and the color pattern is separated into the RGB multi-channels.

In this article, we using a MZJTC correlator system with RLCSLMs and image encoding technique based on the HSV color space for polychromatic pattern recognition. The minimum average correlation energy (MACE) [10] method is also utilized to design the reference functions in the input spatial domain [11]. The concept of image encoding leads to the size of the RLCSLMs will be small by the interlaced rearrangement of hue, saturation and value color components. However, the MACE filter is complex-valued and requires large dynamic range, which is hard to be implemented with presently available RLCSLMs. Consequently, we also utilize the multi-level quantized reference function (MQRF) filter [12] to design the input reference function, which is a spatial domain filter with finite quantization levels. The both techniques can yield sharp

Manuscript received December 12, 2007. This work was supported by the National Science Council in Taiwan, under Grant No. NSC 96-2628-E-155-005-MY3.

Chungcheng Lee is with the department of Electrical Engineering, Yuan Ze university, 135 Yung Tung Road, Taoyuan 32026, Taiwan. phone: +886-3-463-8800 ext 2426; fax: +886-3-463-9355; e-mail: chulung@saturn.yzu.edu.tw.

correlation peaks. At last, the simulation numerical results are obtained to verify our performance of the system.

## II. ANALYSIS

The MZJTC using image encoding technique (IEMZJTC) architecture with RLCSLMs is now used in optical image processing. The implementation setup with interlaced scanned color components is shown in Fig.1. It consists of a laser as a source, a collimated lens (CL), 2 beam splitters (BSs), 3 RLCSLMs, 3 Fourier lenses (FLs), 3 CCD cameras, 1 electronic Subtractor (ES) to remove the zero-order term of JTPS, and a PC to control the whole system. The RLCSLM consists of a polarizing beam splitter (PBS), a half wave plate (HWP), a quarter wave plate (QWP), and a LC modulator.

The RLCSLM1 and RLCSLM2 can display the grayscale images of color components for the encoded reference image and the encoded target image, which are denoted by  $e(x+d, y)$  and  $t(x-d, y)$ , respectively. Here  $d$  is the distance of the reference channel and target channel away from the horizontal central lines of the RLCSLM. The model corresponds better to how people experience color than the RGB color space does. Let small capital letters  $h$ ,  $s$  and  $v$  denote, respectively, the normalized hue, saturation, and value channels in the HSV space, with color values normalized to 1 for full intensity. The HSV color space used to be called the hexcone color model, which is shown in Fig. 2. In general, the system representation of digital color is 8-bits per component. Therefore, digital RGB values are with a range between 0 and 255. Each component can be regarded as a grayscale image. In optics, the component values are normalized, with full intensity, 255, equal to 1.0 for convenience. Let small capital letters  $r$ ,  $g$  and  $b$  denote, respectively, the normalized R, G, and B channels in the RGB space. We can transfer the RGB to HSV color space as the following equations:

$$h = \begin{cases} \frac{\theta}{2\pi} & \text{if } b \leq g \\ \frac{2\pi - \theta}{2\pi} & \text{if } b > g \end{cases} \quad (1)$$

$$\text{with } \theta = \cos^{-1} \left\{ \frac{[(r-g) + (r-b)]}{2[(r-g)^2 + (r-g)(g-b)]^{1/2}} \right\},$$

$$s = \frac{\max(r, g, b) - \min(r, g, b)}{\max(r, g, b)}, \quad (2)$$

and

$$v = \max(r, g, b), \quad (3)$$

where max and min operators select the maximum and

minimum values of the operand, respectively. We can see that the transformation from RGB to HSV is a non-linear operation. Next, the  $h$ ,  $s$ , and  $v$  components will be utilized in our IEMZJTC system with image encoding technique for color image. In this method, these grayscale images are organized as a new encoded image, as shown in Fig. 2, which is displayed on a single, monochromatic, input plane.

The process is listed as follows:

$$1. \text{ Let } h = \begin{bmatrix} h_1 \\ h_2 \\ \vdots \\ h_n \end{bmatrix}, s = \begin{bmatrix} s_1 \\ s_2 \\ \vdots \\ s_n \end{bmatrix}, \text{ and } v = \begin{bmatrix} v_1 \\ v_2 \\ \vdots \\ v_n \end{bmatrix}, \quad (4)$$

where  $h$ ,  $s$ , and  $v$  represent the matrices of hue, saturation, value images, respectively;  $n$  denotes the number of the maximum row vector.

2. Insert one by one respectively each  $h$ ,  $s$ , and  $v$  row vector to a matrix.

$$e = \begin{bmatrix} h_1 \\ s_1 \\ v_1 \\ \vdots \\ h_n \\ s_n \\ v_n \end{bmatrix}. \quad (5)$$

Hence, the new matrix  $e$  is an encoding image, which includes all color elements. This method is different from multi-channel single-output JTC. The encoding image can represent the combination of hue, saturation, and value grayscale images at the input plane. The system could be smaller since the channel number of input image has reduced to a single channel. The encoded reference image and the encoded target image are put into RLCSLM1 and RLCSLM2, respectively. A collimated coherent beam illuminates both the RLCSLM1 and RLCSLM2, and pass through the FLs. We can represent the light fields  $H_1$  and  $H_2$  in terms of the reflected and transmitted components in this IEMZJTC as follows:

$$H_1(\rho, \gamma) = \alpha_1 \cdot E(\rho, \gamma) \cdot \exp\{j2\pi(d\rho)\} + \beta_2 \cdot T(\rho, \gamma) \cdot \exp\{-j2\pi(d\rho)\} \quad (6)$$

and

$$H_2(\rho, \gamma) = \alpha_2 \cdot T(\rho, \gamma) \cdot \exp\{j2\pi(d\rho)\} + \beta_1 \cdot E(\rho, \gamma) \cdot \exp\{-j2\pi(d\rho)\}, \quad (7)$$

where  $\alpha$  and  $\beta$  denote the transmission and reflection coefficients of the BS2, respectively;  $E(\rho, \gamma)$  and  $T(\rho, \gamma)$  are

the Fourier transforms of  $e(x, y)$  and  $t(x, y)$ , respectively;  $\rho$  and  $\gamma$  are mutually independent frequency domain variables. Both of the outputs of CCD1 and CCD2 are connected to an ES. The resultant output of the ES due to the square-law detection is

$$\begin{aligned}
 I_s &= |H_2(\rho, \gamma)|^2 - |H_1(\rho, \gamma)|^2 \\
 &= (|\alpha_1|^2 - |\beta_1|^2) \cdot \{T(\rho, \gamma) \cdot \exp[-j2\pi(d\rho)]\} \\
 &\quad \cdot \{T(\rho, \gamma) \cdot \exp[-j2\pi(d\rho)]\}^* \\
 &+ (|\beta_2|^2 - |\alpha_2|^2) \cdot \{E(\rho, \gamma) \cdot \exp[j2\pi(d\rho)]\} \\
 &\quad \cdot \{E(\rho, \gamma) \cdot \exp[j2\pi(d\rho)]\}^* \\
 &+ (\alpha_1\beta_2^* - \beta_1\alpha_2^*) \cdot \{T(\rho, \gamma) \cdot \exp[-j2\pi(d\rho)]\} \\
 &\quad \cdot \{E(\rho, \gamma) \cdot \exp[j2\pi(d\rho)]\}^* \\
 &+ (\beta_2\alpha_1^* - \alpha_2\beta_1^*) \cdot \{E(\rho, \gamma) \cdot \exp[j2\pi(d\rho)]\} \\
 &\quad \cdot \{T(\rho, \gamma) \cdot \exp[-j2\pi(d\rho)]\}^* .
 \end{aligned} \tag{8}$$

According to Stokes relations [13], let  $\beta_2 = -\beta_1$ ,  $|\alpha_1| = |\beta_1|$ , and  $|\alpha_2| = |\beta_2|$ . We can obtain

$$\begin{aligned}
 I_s &= 2|\beta_2\alpha_1^* + \alpha_1\beta_1^*| \cdot |E(\rho, \gamma)| \cdot |T(\rho, \gamma)| \\
 &\quad \cdot \cos\{2\pi[2d\rho] + \phi + \phi_E(\rho, \gamma) - \phi_T(\rho, \gamma)\},
 \end{aligned} \tag{9}$$

where  $\phi$  is the phase of  $\beta_2\alpha_1^* + \alpha_1\beta_1^*$ ;  $\phi_E$  and  $\phi_T$  are the phases of  $E(\rho, \gamma)$  and  $T(\rho, \gamma)$  respectively. Finally, the MZJTPS can be obtained without the zero-order term. Then, we display  $I_s$  in RLCSLM3. Finally, we can obtain the intensity distribution without auto-correlation term at the output correlation plane via the CCD3 detector, which is

$$\begin{aligned}
 I_s(x, y) &= |c(-x, -y)|^2 \otimes \delta(x + 2d, y) \\
 &\quad + |c(x, y)|^2 \otimes \delta(x - 2d, y) ,
 \end{aligned} \tag{10}$$

where  $c(x, y) = e(x, y) \circ t(x, y)$  is the complex cross-correlation between  $e$  and  $t$ ;  $\circ$  and  $\otimes$  denote the correlation and convolution operations, respectively. Furthermore, we can minimize the average correlation energy for all training images by using the Lagrange multipliers method and constrain the correlation peak to be a desired value  $P$ . The optimum solution can be depicted as the following equation.

$$\hat{E} = \hat{D}^{-1} \hat{T} [(\hat{T}^*)^T \hat{D}^{-1} \hat{T}]^{-1} \hat{P}^* . \tag{11}$$

The solution in (11) is a vector representation in the frequency domain. After the column vector  $\hat{E}$  is rearranged as a square matrix  $E(\rho, \gamma)$ ,  $e(x, y)$  can be obtained by inverse Fourier transform of  $E(\rho, \gamma)$ ; that is

$$e(x, y) = \mathfrak{F}^{-1}\{E(\rho, \gamma)\} . \tag{12}$$

Moreover, the MQRF is used to obtain the quantized function with finite levels in this IEMZJTC system. The transmittance is controlled with digital voltages and is therefore quantized because the commercial LCD circuit is designed with digital IC technology. Finally, the Eq. (12) with MQRFs can be expressed as

$$e(x, y) = \frac{1}{2^Q} \text{Round}\left(\frac{\mathfrak{F}^{-1}[E(\rho, \gamma)]}{M} 2^Q\right), \tag{13}$$

where  $M$  is the maximum of  $|\mathfrak{F}^{-1}[E_k(\rho, \gamma)]|$ ;  $Q$  is the amplitude quantization parameter;  $\text{Round}(K)$  function rounds  $K$  to the nearest integer. Since the reference function is real-valued in the spatial domain, the RLCSLM device in the IEMZJTC requires real-valued only modulation.

### III. SIMULATION RESULTS

The performance of the IEMZJTC based on the HSV color space is investigated with the MQRF. We chose a colorful fish image with  $128 \times 128$  pixels as the test image, which is shown as Fig. 2. Furthermore, we utilize the combination of  $h$ ,  $s$ , and  $v$  grayscale images to form an encoded image with  $384 \times 128$  pixels. Furthermore, we utilize the combination of  $h$ ,  $s$ , and  $v$  grayscale images to form an encoded image with  $384 \times 128$  pixels. The training set also contains 25 color images with different angles of in-plane rotation for simplicity. The rotational distortion range from  $-24^\circ$  to  $24^\circ$  is considered (in steps of  $2^\circ$ ). Next, we synthesize the reference image from training images set with the methods of Lagrange multipliers and the MQRF. The computed reference function for training encoded images with MQRF is put in the RLCSLM1. We choose the  $0^\circ$  rotated image to be the target image, and put the HSV channels of target image in the RLCSLM2. The three-dimensional correlation intensity profiles for the 1st, 2nd, and 5th order quantization levels are illustrated in Figs. 3(a), 3(b), and 3(c), respectively. Accordingly, we can observe the variation of sidelobes under quantization levels  $Q=1$ ,  $Q=2$ , and  $Q=5$ .

From the three-dimensional output profile, we can see that the desired sharp correlation peaks can be seen clearly. Therefore, the system with IEMZJTC based on the HSV color space with quantization method can yield acceptable result to recognize color patterns.

### IV. CONCLUSIONS

In this paper, we have presented a novel optoelectronic system with image encoding technique for invariant color pattern recognition based on the HSV color space. Compared to multi-channel JTC in the joint input plane, the proposed IEMZJTC could be easier and the system could be smaller since the channels of input image can be reduced to a single channel. Besides, the IEMZJTC system can remove the zero-order term in one step without two or more redundant procedures. For real-time processing, the joint input plane is displayed on the RLCSLMs with the MQRF technique to design the reference

function for color pattern recognition. The MQRF with a limited number of discrete levels can be implemented in current available RLCSLMs. Besides, we have proved that the designed reference function is a real-valued function. Meanwhile, some RLCSLM devices are utilized to achieve real-valued only modulation. In the tests, the algorithm is robust to the real-time process and distortion invariance. It is expected that the proposed method is promising in practical applications. Beside, the IEMZJTC based on the HSV color space with MQRFs has quite good performance for polychromatic pattern recognition. To summarize, the overall performances of this IEMZJTC system using MQRFs are good, which offers an attractive alternative for polychromatic pattern recognition.

REFERENCES

[1] A. Vanderlugt, "Signal detection by complex spatial filtering," *IEEE Trans. Inf. Th.*, vol. IT-10, 1964, pp. 139-146.  
 [2] C. S. Weaver and J. W. Goodman, "A technique for optically convolving two functions," *Appl. Opt.*, vol. 5, 1966, pp. 1248-1249.  
 [3] G. Lu, Z. Zhang, S. Wu, and F. T. S. Yu, "Implementation of a nonzero order joint transform correlator by use of phase shifting techniques," *Appl. Opt.*, vol. 36, 1997, pp. 470-483.

[4] C. Li, S. Yin and F. T. S. Yu, "Nonzero-order joint transform correlator," *Opt. Eng.*, vol. 37, 1998, pp. 58-65.  
 [5] C. Cheng and H. Tu, "Implementation of a nonzero-order joint transform correlator using interferometric technique," *Opt. Rev.*, vol. 9, 2002, pp. 193-196.  
 [6] B. Javidi and C. J. Kuo, "Joint transform image correlation using a binary spatial light modulator at the Fourier plane," *Appl. Opt.*, vol. 27, 1988, pp. 663-665.  
 [7] F. T. S. Yu, G. Lu, M. Lu, and D. Zhao, "Application of position encoding to complex joint transform correlator," *Appl. Opt.*, vol. 34, 1995, pp. 1386-1388.  
 [8] C. Wu, C. Chen, and J. Fang, "Linearly constraint color pattern recognition with a nonzero order joint transform correlator," *Opt. Commun.*, vol. 214, 2002, pp. 65-75.  
 [9] M. Deutsch, J. Garcia, and D. Mendlovic, "Multi-channel single-output color pattern recognition by use of a joint-transform correlator," *Appl. Opt.*, vol. 35, 1996, pp. 6976-6982.  
 [10] A. Mahalanobis, B. V. K. V. Kumar, and D. Casasent, "Minimum average correlation energy filters," *App. Opt.*, vol. 26, 1987, pp. 3633-3640.  
 [11] C. Chen, C. Chen, C. Lee, and C. Chen, "Constrained optimization on the nonzero order joint transform correlator constructed with the Mach-Zehnder configuration," *Opt. Commun.*, vol. 231, 2004, pp. 165-173.  
 [12] J. Fang and C. Chen, "Non-zero order joint transform correlator with multi-level quantized reference function," *Opt. Commun.*, vol. 220, 2003, pp. 41-47.  
 [13] E. Hecht, "Optics," Reading, Mass., 4th edition, Addison-Wesley, 2002, pp. 136-137.

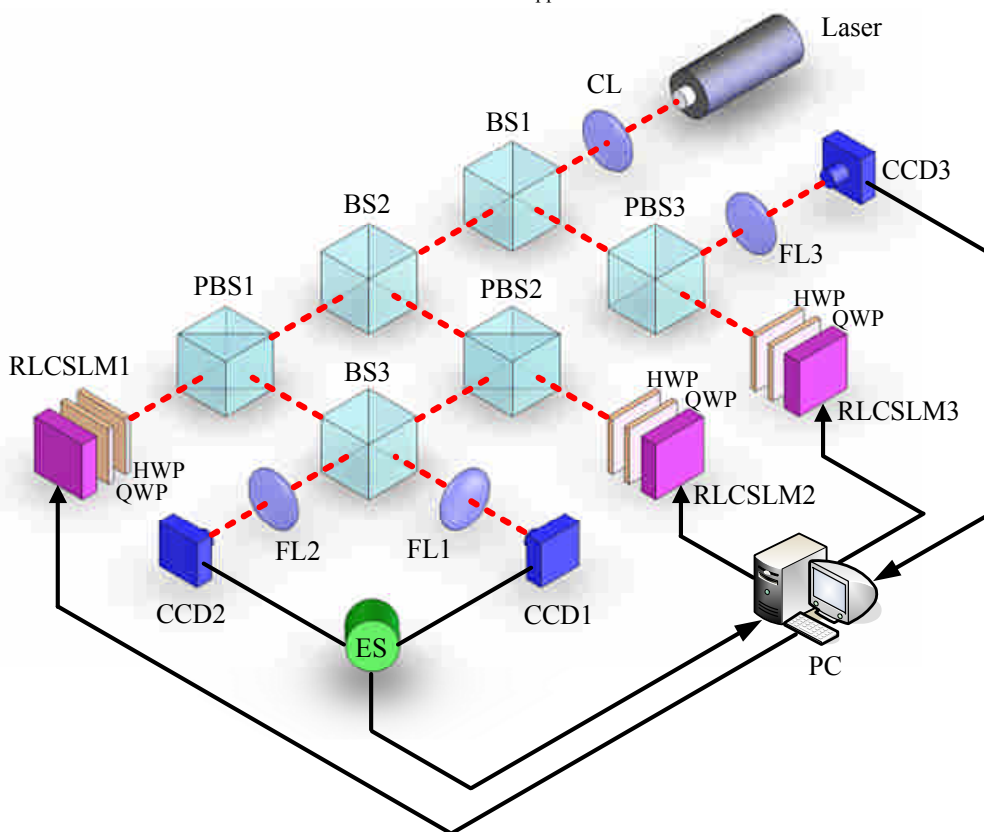


Fig. 1. The schematic diagram of an IEMZJTC system with RLCSLMs.

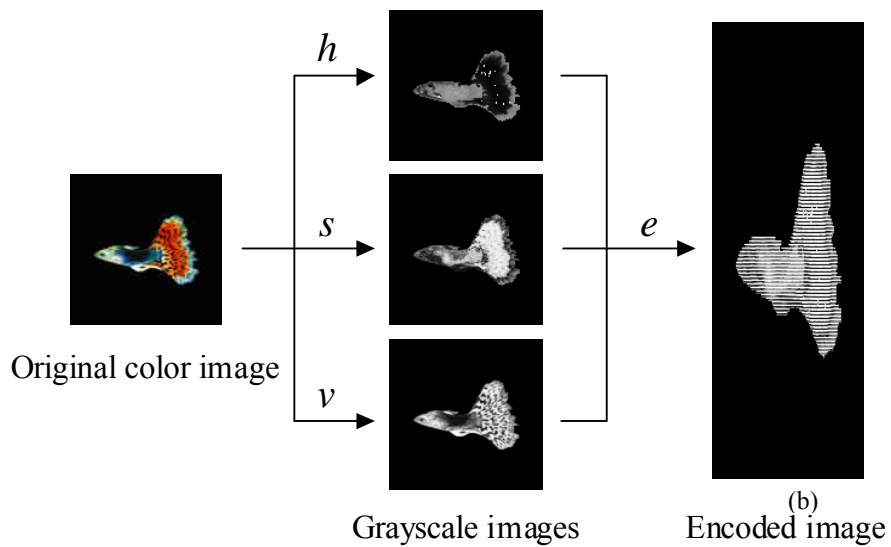


Fig. 2. Image encoding processing with HSV color space in the IEMZJTC

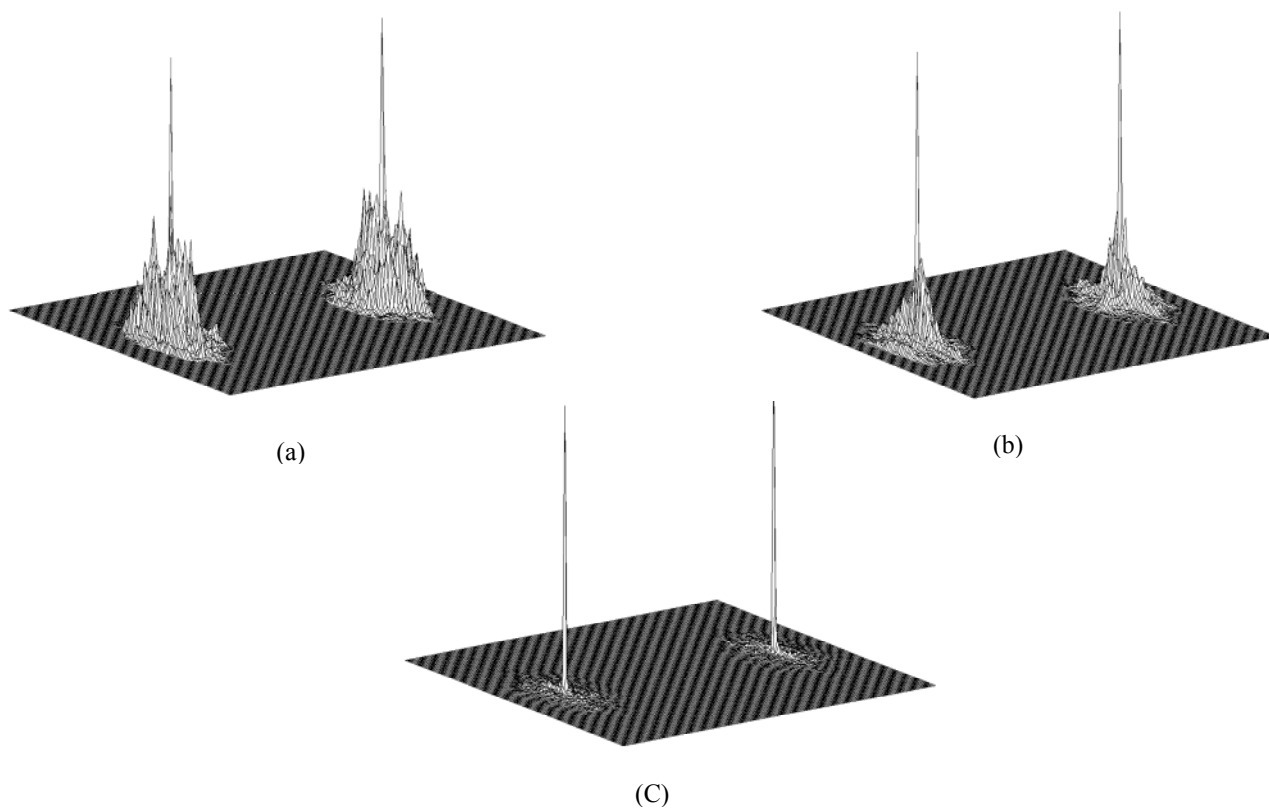


Fig. 3. The 3D correlation intensity profiles with (a)  $Q=1$ , (b)  $Q=2$ , and (c)  $Q=5$ .